ELSEVIER

Biophysical Chemistry 113 (2005) 17–23

Biophysical Chemistry

www.elsevier.com/locate/bpc

A model of intracellular Ca^{2+} oscillations based on the activity of the intermediate-conductance Ca^{2+}-activated K^+ channels

Bernard Fioretti, Fabio Franciolini, Luigi Catacuzzeno*

Dipartimento di Biologia Cellulare e Molecolare Universita' di Perugia via Pascoli 1, I-06123 Perugia, Italy

Received 5 February 2004; received in revised form 15 July 2004; accepted 21 July 2004
Available online 3 September 2004

Abstract

Intracellular Ca^{2+} oscillations are observed in a large number of non-excitable cells. While most appear to reflect an intermittent Ca^{2+} release from intracellular stores, in some instances intracellular Ca^{2+} oscillations strongly depend on Ca^{2+} influx, and are coupled to oscillations of the membrane potential, suggesting that a plasma membrane-based mechanism may be involved. We have developed a theoretical model for the latter type of intracellular Ca^{2+} oscillations based on the Ca^{2+}-dependent modulation of the intermediate-conductance, Ca^{2+}-activated K^+ (IK_{Ca}) channel. The functioning of this model relies on the Ca^{2+}-dependent activation, and the much slower Ca^{2+}-dependent rundown of this channel. We have shown that Ca^{2+}-dependent activation of the IK_{Ca} channels, the consequent membrane hyperpolarization and the resulting increase in Ca^{2+} influx may confer the positive feedback mechanism required for the ascending phase of the oscillation. The much slower Ca^{2+}-dependent rundown process will conversely halt this positive loop, and establish the descending phase of the intracellular Ca^{2+} oscillation. We found that this simple model gives rise to intracellular Ca^{2+} oscillations when using physiologically reasonable parameters, suggesting that IK_{Ca} channels could participate in the generation of intracellular Ca^{2+} oscillations.

Keywords: Calcium oscillations; Intermediate-conductance potassium channels; Theoretical model

1. Introduction

Oscillations of the intracellular Ca^{2+} concentration ($[Ca^{2+}]_i$) have been reported in a variety of non-excitable cells (reviewed in Ref. [1]), and appear to be important in the control of several cell activities, such as energy metabolism, secretion, gene transcription, and the regulation of kinases and phosphatases [2–5]. $[Ca^{2+}]_i$ oscillations are often triggered by physiologically relevant concentrations of phospholipase C (PLC)-coupled agonists. This fact has led many investigators to conclude that the underlying mechanism is the Ca^{2+}-induced Ca^{2+}-release (CIRC) from intracellular stores. Moreover, removal of extracellular Ca^{2+} or changes in membrane potential have been shown to have no effect on the $[Ca^{2+}]_i$ oscillations for several cycles in most of the cell types investigated [6,7]. Based on these observations $[Ca^{2+}]_i$ oscillations have been modelled as being the result of an intermittent Ca^{2+} release from intracellular stores which is often determined by the CIRC mechanism (reviewed in Ref. [8]). In this case, the basic underlying processes of the $[Ca^{2+}]_i$ oscillations are confined to the interior of the cell and the Ca^{2+} entry is only required to replenish the intracellular Ca^{2+} stores.

In some cells, however, $[Ca^{2+}]_i$ oscillations do not conform to the above scheme, rather they are generated by plasmalemma-based mechanisms, such as oscillatory changes in the rate of Ca^{2+} entry [2,9–13]. In activated T lymphocytes, for example, the thapsigargin-induced $[Ca^{2+}]_i$ oscillations are rapidly inhibited by a reduced Ca^{2+} influx, achieved either by reducing extracellular $[Ca^{2+}]$, or by blocking Ca^{2+} influx pathways. $[Ca^{2+}]_i$ oscillations have also been found to be correlated with oscillations of the membrane potential, which is a major determinant of the driving force for Ca^{2+} influx [9,10,12–14]. In several

* Corresponding author. Tel.: +39 75 585 5750; fax: +39 75 585 5762.
E-mail address: fabiolab@unipg.it (L. Catacuzzeno).

0301-4622/$ - see front matter © 2004 Elsevier B.V. All rights reserved.
doi:10.1016/j.bpc.2004.07.037

instances, it has been demonstrated that if the rhythmic changes of membrane potential are stopped, the Ca^{2+} oscillatory response disappears [12,13,15]. This fact suggests that $[Ca^{2+}]_i$ oscillations may be generated by the oscillatory changes in the rate of Ca^{2+} entry, and further supports the hypothesis of an underlying plasma membrane-based mechanism. The above data have stimulated our search for a theoretical model in which plasmalemma-based (as opposed to intracellular confined) mechanisms are central to the generation of $[Ca^{2+}]_i$ oscillations. The model here proposed is based on a dual Ca^{2+}-dependent modulation of the intermediate-conductance, Ca^{2+}-activated K^+ (IK_{Ca}) channels (see below).

Calcium-activated K^+ (K_{Ca}) channels participate in a multitude of physiological processes by coupling intracellular Ca^{2+} signalling to membrane voltage. Traditionally, K_{Ca} channels have been classified as large (BK), small (SK), and intermediate (IK_{Ca}), based on their single channel conductance [16,17]. IK_{Ca} channels are expressed primarily by non-excitable cells, including secretory epithelia [18], erythrocytes [19], lymphocytes [20], and glioma cells [21]. IK_{Ca} channels are activated by $[Ca^{2+}]_i$ with an IC_{50} of several hundred nanomolars, well within the range of $[Ca^{2+}]_i$ reached during $[Ca^{2+}]_i$ oscillations. A less well investigated characteristic of the IK_{Ca} channels is its Ca^{2+}-dependent rundown, having kinetics much slower than its Ca^{2+}-dependent activation. In several cells, IK_{Ca} current activation, usually induced by bath application of ionomycin or cell dialysis with a high $[Ca^{2+}]_i$ solution, is followed by a slow inactivation of the current [22–24]. This process is also present when recordings are made using the perforated-patch configuration which preserves cell integrity, indicating that channel rundown is not due to the loss of intracellular factors [23,24]. Current rundown is accelerated with increasing $[Ca^{2+}]_i$, suggesting that the process is Ca^{2+}-dependent [24]. Notably, cells exhibiting synchronized oscillations of $[Ca^{2+}]_i$ and membrane potential abundantly express IK_{Ca} channels [9,10,13,25]. Furthermore, blockage of IK_{Ca} channels with charybdotoxin leads to the inhibition of $[Ca^{2+}]_i$ oscillations in both C6 glioma cells [13] and T lymphocytes [15], suggesting that the activity of IK_{Ca} channels is essential for the generation of these oscillatory activities.

We reasoned that the Ca^{2+}-dependent activation of IK_{Ca} channels, the consequent membrane hyperpolarization and the increase in Ca^{2+} influx may provide the positive feedback needed during the ascending phase of the $[Ca^{2+}]_i$ oscillation (Fig. 1A). The much slower Ca^{2+}-dependent rundown could, conversely, interrupt this positive loop, and establish the descending phase of the $[Ca^{2+}]_i$ oscillatory cycle. The model presented below tests whether IK_{Ca} channels could potentially be the key component of a plasma membrane-based $[Ca^{2+}]_i$ oscillatory activity.

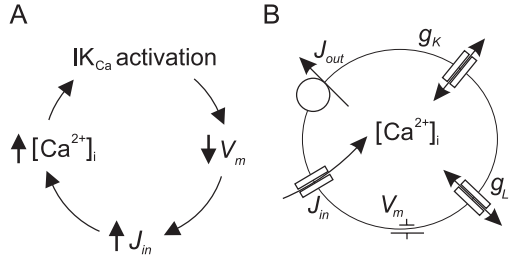

Fig. 1. The model of $[Ca^{2+}]_i$ oscillations based on the IK_{Ca} channel activity. (A) Positive feedback loop controlling $[Ca^{2+}]_i$, that involves IK_{Ca} channel activation by the intracellular Ca^{2+}, membrane hyperpolarizarion and the consequent increase in Ca^{2+} influx. (B) Scheme illustrating the various plasmalemmal components included in our model. Symbols have the following meaning: J_{out}, energy-driven Ca^{2+} flux out of the cell; J_{in}, inward Ca^{2+} flux driven by the electrochemical gradient; $[Ca^{2+}]_i$, intracellular Ca^{2+} concentration; V_m, transmembrane potential difference (inside minus outside); g_L, leakage conductance; g_K, IK_{Ca} conductance.

2. Mathematical model

Fig. 1B depicts the cellular components included in our model of $[Ca^{2+}]_i$ oscillations. Two plasma membrane-based mechanisms contribute to alterations in the $[Ca^{2+}]_i$, here referred to as x: a passive Ca^{2+} influx through a voltage-independent pathway (J_{in}), and an energy-driven Ca^{2+}-extrusion from the cytosol to the extracellular medium (J_{out}):

$$\frac{dx(t)}{dt} = \frac{J_{in} - J_{out}}{vol} \tag{1}$$

vol represents the cell volume, corrected for the buffering capacity of the intracellular medium (see, for example, Ref. [26]). J_{in} is driven by the membrane potential difference between the inside and outside of the cell, V_m, in accordance with the following ohmic relationship (see, for example, Ref. [27]):

$$J_{in} = -\frac{g_{Ca}(V_m - E_{Ca})}{z_{Ca}F} \tag{2}$$

where g_{Ca}, E_{Ca}, and z_{Ca} are the Ca^{2+} conductance, reversal potential, and valence, respectively, and F is the Faraday constant.

The energy-driven Ca^{2+} extrusion from the cytosol to the extracellular medium, J_{out}, is modelled as a membrane Ca^{2+}-ATPase activity (see, for example, Refs. [28,29]):

$$J_{out} = \phi_{Ca}\frac{x^2}{x^2 + K_{out}^2} \tag{3}$$

where ϕ_{Ca} is the maximal activity of the pump and K_{out} its Ca^{2+} dissociation constant.

V_m is set by the ionic conductances present in the membrane. Besides the above described g_{Ca}, we also included in the model a leakage conductance (g_L) and a K^+ conductance (g_K) (see Fig. 1B). The leakage conductance includes the contribution of the different cation and anion background channels present in the cell. The electro-

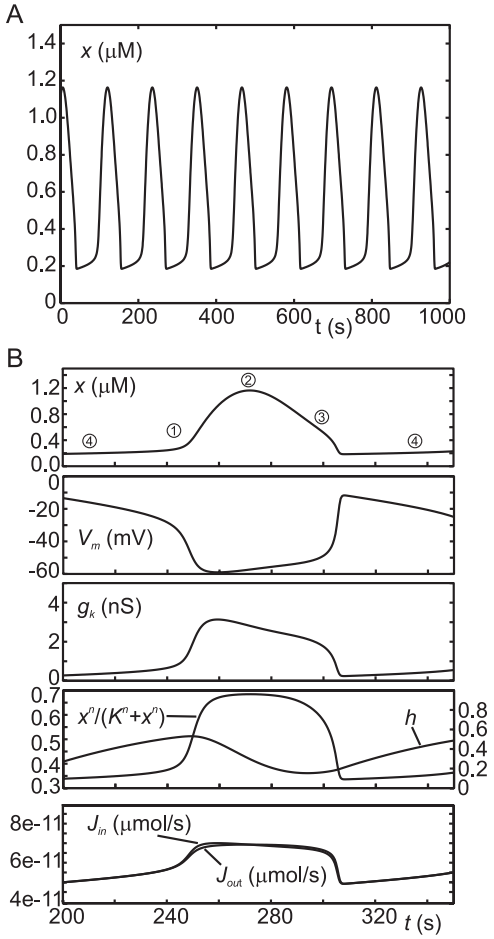

Fig. 2. Anatomy of the $[Ca^{2+}]_i$ oscillations. (A) $[Ca^{2+}]_i$ oscillations generated by numerical integration of the model described in this paper. The model parameters are reported in Table 1. (B) Time course of changes in the relevant variables of the model during the $[Ca^{2+}]_i$ oscillatory cycle.

neutrality condition imposes that the transmembrane total ion current is zero, namely:

$$g_L(V_m - E_L) + g_{Ca}(V_m - E_{Ca}) + g_K(V_m - E_K) + J_{out}\,F = 0 \quad (4)$$

where E_L and E_K are the leakage and K^+ reversal potentials, respectively. The term $J_{out}\,F$ takes into account the contribution of the Ca^{2+}-ATPase to the transmembrane current, assuming a Ca^{2+}/H^+ countertransport with a stoichiometry of 1:1 [30]. Eq. (4) can be solved to give a relationship for membrane voltage

$$V_m = \frac{g_{Ca}E_{Ca} + g_L E_L + g_K E_K - J_{out}F}{g_{Ca} + g_L + g_K} \quad (5)$$

Note that in Eqs. (4) and (5) the membrane charging (capacitance) current has been neglected, assuming that it is fast compared to the time scale of $[Ca^{2+}]_i$ oscillations.

The key feature of our model is the double, antagonistic modulation (positive and negative) of g_K (here represented by the IK_{Ca} channels) that occurs with significantly different kinetics: the Ca^{2+}-dependent activation, and the much slower, Ca^{2+}-dependent current rundown. Namely

$$g_K = g_{K,\,max}\,h(t)\,\frac{x^n}{x^n + K^n} \quad (6)$$

where $g_{K,max}$ is the maximal IK_{Ca} conductance, $h(t)$ represents the time-dependent fraction of available channels (not residing in the rundown state), and K and n are the Ca^{2+} binding constant and Hill coefficient for the Ca^{2+}-dependent channel activation, respectively. Note that while the Ca^{2+}-dependent IK_{Ca} channel activation is considered instantaneous on the temporal scale of the $[Ca^{2+}]_i$ oscillations, the rundown process is instead much slower. In the absence of experimental evidence regarding the kinetic mechanism underlying IK_{Ca} channel rundown, we modelled this process as a first-order, Ca^{2+}-dependent transition, namely

$$''h'' \underset{k_{-1}}{\overset{k_1[Ca^{2+}]_i}{\rightleftarrows}} ''1-h'' \quad \text{(Scheme1)}$$

where "h" and "$1-h$" represent the channel not-residing and residing in the rundown state, respectively, and k_1 and k_{-1} are the forward and reverse rate constant for channel rundown. In accordance with Scheme 1, the temporal evolution of rundown is described by the following first-order differential equation, generally used to describe the dynamics of activation and inactivation of ion channel gates [31]:

$$\frac{dh(t)}{dt} = k_1 K_h[1 - h(t)] - k_1 x(t) h(t) \quad (7)$$

where $K_h = k_{-1}/k_1$ is the dissociation constant for Ca^{2+} ions.

3. Results

Fig. 2A shows that our model, seeded with reasonable values of the cell parameters (see Table 1), is able to respond with sustained $[Ca^{2+}]_i$ oscillations. To try to understand the mechanism(s) underlying the oscillatory activity, we looked at the temporal variations of the relevant variables during the oscillatory cycle (Fig. 2B). The rising phase of the oscillation (labelled 1 in Fig. 2B) is the result of the positive feedback involving the Ca^{2+}-dependent gating of IK_{Ca} channels and membrane potential (cf. Fig. 1A). During this phase, raising $[Ca^{2+}]_i$ increases the open probability of the IK_{Ca} channel. This results in a hyperpolarization of the membrane which will increase the electrochemical gradient for Ca^{2+} influx,

Table 1
Parameter values of the model

$g_{K,max}$=7 nS	E_{Ca}=0.1 V
n=3	g_L=1 nS
K=400 nM	E_L=0 V
K_h=400 nM	K_p=120 nM
E_K=−0.08 V	ϕ_{Ca}=0.7×10^{-16} mol/s
k_1=2×10^4 s^{-1} M^{-1}	z_{Ca}=2
g_{Ca}=85 pS	vol=30 pL

leading to a further increase in $[Ca^{2+}]_i$. The rising phase in $[Ca^{2+}]_i$ terminates (phase 2) when sufficient time has elapsed to get a sensible rundown of IK_{Ca} channels, which will cause a membrane repolarization and a reduction in Ca^{2+} influx. Under these conditions, Ca^{2+} pumps will slowly deplete the intracellular Ca^{2+}, causing the descending phase of the oscillation (phase 3). Finally, IK_{Ca} channels will recover from rundown (phase 4) when low $[Ca^{2+}]_i$ conditions are re-established, allowing the cycle to start over again.

We next investigated the dependence of the model on the IK_{Ca} channel properties (Figs. 3 and 4). This was done by using the program XPPAUT as implemented by B. Ermentrout (http://www.math.pitt.edu/~bard/xpp/xpp.html). Fig. 3A presents a bifurcation diagram showing the steady states and oscillatory solutions, as well as their stability, as the maximal IK_{Ca} conductance, $g_{K,max}$, is varied. Fig. 3B (a–d) shows phaseplane diagrams for four different $g_{K,max}$ values, corresponding to the four different behaviors encountered in panel A. For $g_{K,max}$ values lower than 5.6 nS there is a single steady state representing a globally stable attractor. As shown in the phaseplane diagram of Fig. 3B(a), made up with a $g_{K,max}$ value within this region, model trajectories will decay towards this steady state. With larger $g_{K,max}$ values the steady state loose stability in a Hopf bifurcation. For $g_{K,max}$ values just above this point the trajectory will end in a stable limit cycle (see the phaseplane diagram of Fig. 3B(b)). Finally, the fixed point gains again stability in another Hopf bifurcation at $g_{K,max}$=7.1 nS, and remain stable as $g_{K,max}$ continues to increase (Fig. 3A). The upper Hopf bifurcation is subcritical, and the resultant branch of unstable periodic orbits (open symbols in Fig. 3A) turns around in a saddle node of periodic bifurcation (at $g_{K,max}$=8.3 nS), giving rise to a branch of stable limit cycles (closed symbols in Fig. 3A). In the range of $g_{K,max}$ values between the upper Hopf bifurcation and the saddle node of periodic bifurcation, the model is actually bistable, generating either sustained $[Ca^{2+}]_i$ oscillations or a stable $[Ca^{2+}]_i$, depending on the initial conditions of the simulation. This behavior can be better understood by looking at the corresponding phaseplane

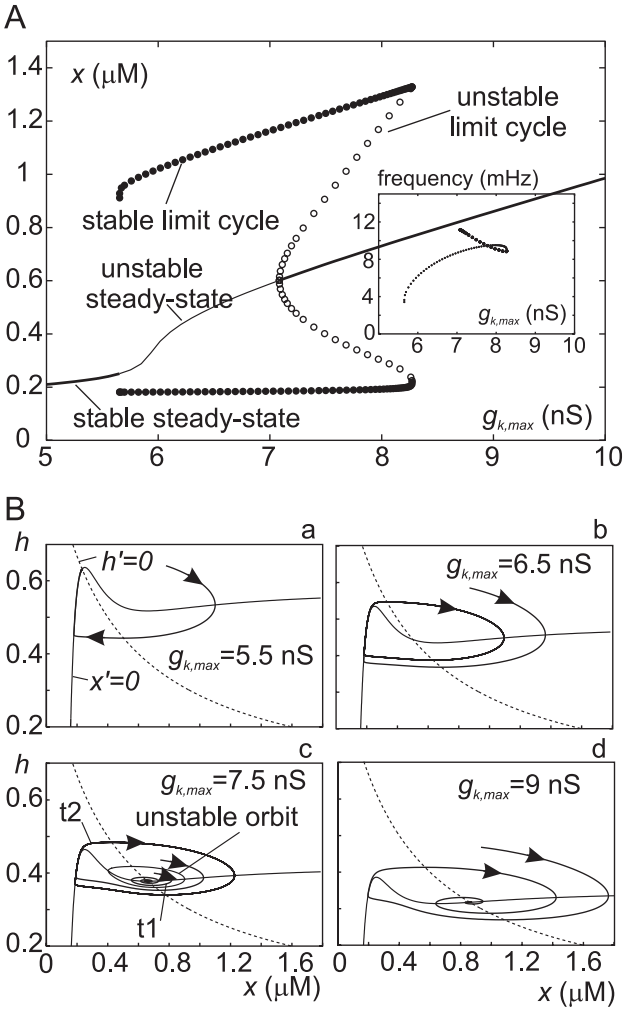

Fig. 3. Dependence of $[Ca^{2+}]_i$ oscillations on the IK_{Ca} conductance. (A) Bifurcation diagram of our model, made with $g_{K,max}$, the maximal IK_{Ca} conductance, as a variable. Solid thick and thin lines indicate stable and unstable steady states, respectively. Closed and open symbols indicate stable limit cycle and unstable orbits, respectively. Inset: plot of the oscillatory frequency as a function of $g_{K,max}$, for both stable limit cycles and unstable periodic orbits. (B) Phaseplane diagrams showing the behavior of the model for four different $g_{K,max}$ values. All the other parameters of the model were held fixed to the values reported in Table 1. Dashed and solid thin lines represent the x- and h-nullcline, respectively, while thick lines denote trajectories.

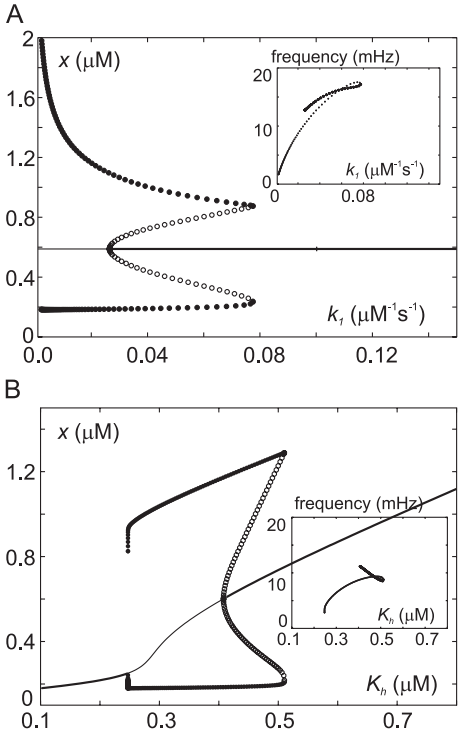

Fig. 4. Dependence of $[Ca^{2+}]_i$ oscillations on the rundown kinetics and steady state properties. Panels (A) and (B): bifurcation diagrams and frequency plots (insets) made by considering k_1, the forward rate constant for channel rundown (A), or K_h, the Ca^{2+} ion dissociation constant for channel rundown (B), as variables. All the other parameters of the model were held fixed to the values reported in Table 1.

diagram shown in Fig. 3B(c). The fixed point of the system here has attracting properties, and trajectories starting close to it are attracted (see the trajectory labelled t1 in the diagram of Fig. 3B(c)). A different behavior is instead obtained for trajectories starting farther away from this fixed point which, rather than being attracted towards the fixed point, ends up in a stable limit cycle (see the trajectory labelled t2 in the diagram of Fig. 3B(c)). The two attractors (the fixed point and the stable limit cycle) are separated by an unstable orbit (marked in the diagram with a thin line), that we have found by backward integration of the system. Initial h and x values inside the unstable orbit tend to the attracting steady state, while initial values outside of it will lead to the limit cycle. Finally, note from the phaseplane diagrams of Fig. 3B that varying $g_{K,max}$ affect only the x-nullcline, while leaving unaltered the h-nullcline, as expected from Eqs. (1) and (7). In the inset of Fig. 1A the oscillatory frequency of the stable and unstable limit cycles are reported as a function of $g_{K,max}$. It can be seen that the oscillatory frequency significantly increases with increasing $g_{K,max}$.

We also found that the rate and steady state properties of IK_{Ca} channel rundown are particularly important to establish the $[Ca^{2+}]_i$ oscillations (Fig. 4A and B). As shown in Fig. 4A, a faster channel rundown (achieved by increasing the forward rate constant, k_1) causes the oscillations to be of lower amplitude and higher frequency (see inset to Fig. 4A). Notably, for k_1>0.077 s^{-1} mM^{-1} the oscillatory activity disappeared (Fig. 4A). This result suggests that the hysteresis of the IK_{Ca} channel activity (i.e. the significantly different g_K trajectories during the ascending and descending phases of the $[Ca^{2+}]_i$ oscillation), caused by the slow kinetics of channel rundown, is an essential feature for the existence of $[Ca^{2+}]_i$ oscillations.

Fig. 5 finally illustrates the dependence of $[Ca^{2+}]_i$ oscillations on Ca^{2+} influx, namely the parameter g_{Ca}.

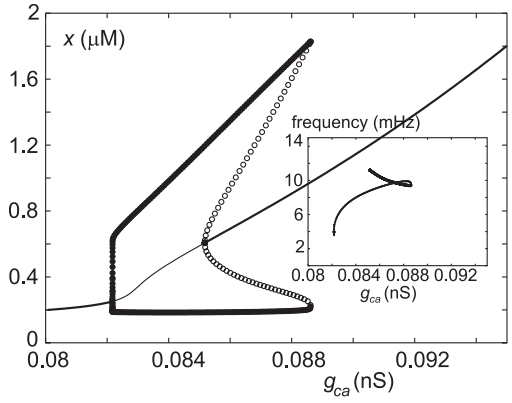

Fig. 5. Dependence of $[Ca^{2+}]_i$ oscillations on Ca^{2+} conductance. Bifurcation diagram of our model, made with g_{Ca}, the Ca^{2+} conductance, as a variable. All the other parameters of the model were held fixed to the values reported in Table 1. Solid thick and thin lines indicate stable and unstable steady states, respectively. Closed and open symbols indicate stable limit cycles and unstable orbits, respectively. Inset: plot of the oscillatory frequency as a function of g_{Ca}, for both stable limit cycles and unstable periodic orbits.

Since PLC-coupled agonists are often able to increase Ca^{2+} entry rate, due to activation of capacitative Ca^{2+} entry as result of agonist-induced Ca^{2+} store depletion, or alternatively to the arachidonic acid (AA)-mediated opening of Ca^{2+}-selective conductances (reviewed in Ref. [32]), variations in the agonist concentration would have an effect similar to that obtained by varying the g_{Ca} parameter. It can be seen that sustained oscillations are obtained within a relatively narrow range of the g_{Ca} parameter (Fig. 5). This result is in line with several experimental reports indicating that $[Ca^{2+}]_i$ oscillations are induced only within a window of agonist concentration [33].

4. Discussion

In this study we found that a simple model of plasma membrane-based Ca^{2+} homeostasis gives rise to $[Ca^{2+}]_i$ oscillations when fed with physiologically reasonable parameter values. The key feature of the model is the dual Ca^{2+}-dependent modulation of IK_{Ca} channels: the Ca^{2+}-dependent activation and the slower Ca^{2+}-dependent rundown. In fact, the slow kinetics of the IK_{Ca} channel rundown introduces hysteresis into the model system which is a basic requirement for all oscillatory processes. The formalism used to describe our model of $[Ca^{2+}]_i$ oscillations shares several features with the Hodgkin–Huxley formalism of plasma membrane electrical excitability [34], and with reduced models of $[Ca^{2+}]_i$ oscillations based on the IP_3 receptor kinetics [8,35]. These are, the activation and (slow) inactivation of an ion channel by a regulatory state variable (voltage in the Hodgkin–Huxley model, and Ca^{2+} in the $[Ca^{2+}]_i$ oscillation models, respectively), which in turn positively modulates the channel activity. The positive feedback between the channel activity and the regulatory state variable is the process that underlies the rising phase of the oscillatory cycle (cf. Fig. 1A), whereas channel inactivation achieved by interrupting this positive loop, is responsible for the descending phase of the oscillation. The present model differs from previously published models of $[Ca^{2+}]_i$ oscillations in that: (i) the positive feedback mechanism needed to generate the oscillatory activity involves the IK_{Ca} channel, instead of the CIRC from the endoplasmic reticulum, and (ii) the membrane potential and Ca^{2+} influx are assigned critical roles.

Although the proposed model is at the moment hypothetical, experimental evidence seems to support its applicability in selected cases. For example, in C6 glioma cells, low concentrations of bradykinin induce synchronized oscillations in the $[Ca^{2+}]_i$ and cell membrane potential, both of which are strongly dependent on transmembrane Ca^{2+} fluxes [13]. Bath application of charybdotoxin, an inhibitor of IK_{Ca} channels, effectively blocks both of these oscillatory activities [13], thereby demonstrating the central role that IK_{Ca} channels play in the generation of $[Ca^{2+}]_i$ (and membrane potential) oscillations. A similar mechanism

may also be relevant in the mitogen- and thapsigargin-induced $[Ca^{2+}]_i$ oscillations observed in activated T lymphocytes. In this preparation the oscillatory activity has been shown to be correlated with the oscillatory transmembrane Ca^{2+} influx [36,37], which is probably the result of membrane potential, and Ca^{2+}-driving force, oscillations [38]. Also in this case IK_{Ca} channel inhibition with charybdotoxin blocked the oscillatory activity [15].

We have demonstrated that Ca^{2+}-dependent rundown of IK_{Ca} channels is important for generating $[Ca^{2+}]_i$ oscillations in our model. This process has been documented in several non-excitable cells (see Introduction). The origin of the IK_{Ca} channel rundown is presently unknown, although AA is a possible candidate. Indeed, at sub-micromolar concentrations AA has been shown to inhibit epithelial and cloned IK_{Ca} channels [18], and a Ca^{2+}-dependent AA increase has been demonstrated in many non-excitable tissues [39,40]. Interestingly, the transient stimulation of epithelial Cl^- secretion by Ca^{2+} agonists has been attributed to a Ca^{2+}-dependent AA production and the consequent block of IK_{Ca} channels [18]. Alternatively, the IK_{Ca} channel rundown could be triggered by a Ca^{2+}-dependent phosphorylation and dephosphorylation of the channel protein. Indeed it has been demonstrated that both PKC- and PKA-mediated phosphorylation can alter the activity of this channel [41,42]. Since experimental studies of the detailed kinetics of IK_{Ca} channel rundown are lacking, in our model we described it as a single-step, Ca^{2+}-dependent process.

For a relatively wide range of $g_{K,max}$ values, the model presented here is bistable, rather than oscillatory (cf. Fig. 3), that is, $[Ca^{2+}]_i$ can either oscillate, or remain stable at a definite steady state value, depending on the previous history of the system. A region of the x–h plane exists (the one delimited by the unstable orbit in Fig. 3B(c)) where a trajectory will be attracted towards the fixed point of the system. If the trajectory jumps outside this region, the system will start to oscillate because it is no longer attracted to the fixed point. The system will keep oscillating until another event brings the trajectory back inside the unstable orbit. This occurrence suggests that the mechanism we propose has the potential to play a major role in the generation of the complex $[Ca^{2+}]_i$ oscillations seen in some cells, which consists of periods of relatively high frequency $[Ca^{2+}]_i$ oscillations separated by periods with stable $[Ca^{2+}]_i$ [43].

Several other structures and mechanisms control $[Ca^{2+}]_i$ in living cells, and shape and modulate $[Ca^{2+}]_i$ oscillations. Our simple model does not include these. The many non-linear processes that could participate in an instability-generating loop include CIRC, desensitization of IP_3 receptors, PLC activation by Ca^{2+}, and Ca^{2+} inhibition of capacitative Ca^{2+} entry. These additional processes were not included into our model because our goal was to test whether IK_{Ca} channels could, by themselves, behave as "pacemakers" for $[Ca^{2+}]_i$ oscillations. The membrane oscillator described in this paper, together with other cellular oscillators, could build more complex $[Ca^{2+}]_i$ oscillations. It has been shown that complex oscillatory phenomena, such as bursting and chaotic $[Ca^{2+}]_i$ oscillations, may arise from the interplay between several instability-generating mechanisms, each of which is capable of producing sustained oscillations [44].

Further experimental evidence is needed to obtain a more complete understanding of the physiological relevance of this model.

Acknowledgement

This work was supported by grants from Italian MURST. We thank Sandy Harper (University of Dundee) and Clara Nucci (University of Perugia) for critical reading of the manuscript.

References

[1] M. Berridge, P. Lipp, M. Bootman, Calcium signalling, Curr. Biol. 9 (1999) 157–159.
[2] R.E. Dolmetsch, K. Xu, R.S. Lewis, Calcium oscillations increase the efficiency and specificity of gene expression, Nature 392 (1998) 933–936.
[3] G. Dupont, A. Goldbeter, CaM kinase II as frequency decoder of Ca^{2+} oscillations, BioEssays 20 (1998) 607–610.
[4] W. Li, J. Llopis, M. Whitney, G. Zlokarnik, R.Y. Tsien, Cell-permeant caged InsP3 ester shows that Ca^{2+} spike frequency can optimize gene expression, Nature 392 (1998) 936–941.
[5] R.S. Lewis, Calcium oscillations in T-cells: mechanisms and consequences for gene expression, Biochem. Soc. Trans. 31 (2003) 925–929.
[6] M.J. Berridge, Inositol trisphosphate and calcium signalling, Nature 361 (1993) 315–325.
[7] J.W. Putney Jr., Excitement about calcium signaling in inexcitable cells, Science 262 (1993) 676–678.
[8] S. Schuster, M. Marhl, T. Hofer, Modelling of simple and complex calcium oscillations. From single-cell responses to intercellular signalling, Eur. J. Biochem. 269 (2002) 1333–1355.
[9] F. Lang, F. Friedrich, E. Kahn, E. Woll, M. Hammerer, S. Waldegger, K. Maly, H. Grunicke, Bradykinin-induced oscillations of cell membrane potential in cells expressing the Ha-ras oncogene, J. Biol. Chem. 266 (1991) 4938–4942.
[10] H.J. Westphale, L. Wojnowski, A. Schwab, H. Oberleithner, Spontaneous membrane potential oscillations in Madin–Darby canine kidney cells transformed by alkaline stress, Pflügers Arch. 421 (1992) 218–223.
[11] J.K. Foskett, D.C. Wong, $[Ca^{2+}]_i$ inhibition of Ca^{2+} release-activated Ca^{2+} influx underlies agonist- and thapsigargin-induced $[Ca^{2+}]_i$ oscillations in salivary acinar cells, J. Biol. Chem. 269 (1994) 31525–31532.
[12] R.E. Laskey, D.J. Adams, M. Cannell, C. van Breemen, Calcium entry-dependent oscillations of cytoplasmic calcium concentration in cultured endothelial cell monolayers, Proc. Natl. Acad. Sci. U. S. A. 89 (1992) 1690–1694.
[13] G. Reetz, G. Reiser, $[Ca^{2+}]_i$ oscillations induced by bradykinin in rat glioma cells associated with Ca^{2+} store-dependent Ca^{2+} influx are controlled by cell volume and by membrane potential, Cell Calcium 19 (1996) 143–156.
[14] H. Oberleithner, A. Schwab, H.J. Westphale, L. Wojnowski,

Oscillations: a key event in transformed renal epithelial cells, Clin. Investig. 70 (1992) 816–824.
[15] J.A. Verheugen, F. Le Deist, V. Devignot, H. Korn, Enhancement of calcium signaling and proliferation responses in activated human T lymphocytes. Inhibitory effects of K^+ channel block by charybdotoxin depend on the T cell activation state, Cell Calcium 21 (1997) 1–17.
[16] C. Vergara, R. Latorre, N.V. Marrion, J.P. Adelman, Calcium-activated potassium channels, Curr. Opin. Neurobiol. 8 (1998) 321–329.
[17] R. Latorre, A. Oberhauser, P. Labarca, O. Alvarez, Varieties of calcium-activated potassium channels, Annu. Rev. Physiol. 51 (1989) 385–399.
[18] D.C. Devor, R.A. Frizzell, Modulation of K^+ channels by arachidonic acid in T84 cells: I. Inhibition of the Ca^{2+}-dependent K^+ channel, Am. J. Physiol. 274 (1998) C138–C148.
[19] C. De Brugnara, C.C. Armsby, L. De Franceschi, M. Crest, M.F. Euclaire, S.L. Alper, Ca(2+)-activated K^+ channels of human and rabbit erythrocytes display distinctive patterns of inhibition by venom peptide toxins, J. Membr. Biol. 147 (1995) 71–82.
[20] R.K. Rader, L.E. Kahn, G.D. Anderson, C.L. Martin, K.S. Chinn, S.A. Gregory, T cell activation is regulated by voltage-dependent and calcium-activated potassium channels, J. Immunol. 156 (1996) 1425–1430.
[21] D. Manor, N. Moran, Modulation of small conductance calcium-activated potassium channels in C6 glioma cells, J. Membr. Biol. 140 (1994) 69–79.
[22] Y. Huang, S.G. Rane, Potassium channel induction by the Ras/Raf signal transduction cascade, J. Biol. Chem. 269 (1994) 31183–31189.
[23] H.J. Draheim, H. Repp, F. Dreyer, Src-transformation of mouse fibroblasts induces a Ca^{2+}-activated K^+, current without changing the T-type Ca^{2+} current, Biochim. Biophys. Acta 1269 (1995) 57–63.
[24] X. Lu, A. Fein, M.B. Feinstein, F.A. O'Rourke, Antisense knock out of the inositol 1,3,4,5-tetrakisphosphate receptor GAP1(IP4BP) in the human erythroleukemia cell line leads to the appearance of intermediate conductance K_{Ca} channels that hyperpolarize the membrane and enhance calcium influx, J. Gen. Physiol. 113 (1999) 81–96.
[25] A. Schwab, H.J. Westphale, L. Wojnowski, S. Wunsch, H. Oberleithner, Spontaneously oscillating K^+ channel activity in transformed Madin–Darby canine kidney cells, J. Clin. Invest. 92 (1993) 218–223.
[26] T. Hofer, Model of intercellular calcium oscillations in hepatocytes: synchronization of heterogeneous cells, Biophys. J. 77 (1999) 1244–1256.
[27] M.S. Jafri, S. Vajda, P. Pasik, B. Gillo, A membrane model for cytosolic calcium oscillations. A study using Xenopus oocytes, Biophys. J. 63 (1992) 235–246.
[28] M.V. Martinov, V.M. Vitvitsky, F.I. Ataullakhanov, Volume stabilization in human erythrocytes: combined effects of Ca^{2+}-dependent potassium channels and adenylate metabolism, Biophys. Chem. 80 (1999) 199–215.
[29] D.M. Bautista, M. Hoth, R.S. Lewis, Enhancement of calcium signalling dynamics and stability by delayed modulation of the plasma-membrane calcium-ATPase in human T cells, J. Physiol. 541 (2002) 877–894.
[30] J.M. Salvador, G. Inesi, J.L. Rigaud, A.M. Mata, Ca^{2+} transport by reconstituted synaptosomal ATPase is associated with H^+ countertransport and net charge displacement, J. Biol. Chem. 273 (1998) 18230–18234.
[31] B. Hille, Ionic Channels of Excitable Membranes, Sinauer Associates, Suderland, MA, 1992.
[32] T.J. Shuttleworth, O. Mignen, Calcium entry and the control of calcium oscillations, Biochem. Soc. Trans. 31 (2003) 916–919.
[33] A. Goldbeter, Computational approaches to cellular rhythms, Nature 420 (2002) 238–245.
[34] A.L. Hodgkin, A.F. Huxley, A quantitative description of membrane current and its application to conduction and excitation in nerve, J. Physiol. 117 (1952) 500–544.
[35] Y.X. Li, J. Rinzel, Equations for InsP3 receptor-mediated $[Ca^{2+}]_i$ oscillations derived from a detailed kinetic model: a Hodgkin–Huxley like formalism, J. Theor. Biol. 166 (1994) 461–473.
[36] S.D. Hess, M. Oortgiesen, M.D. Cahalan, Calcium oscillations in human T and natural killer cells depend upon membrane potential and calcium influx, J. Immunol. 150 (1993) 2620–2633.
[37] R.E. Dolmetsch, R.S. Lewis, Signaling between intracellular Ca^{2+} stores and depletion-activated Ca^{2+} channels generates $[Ca^{2+}]_i$ oscillations in T lymphocytes, J. Gen. Physiol. 103 (1994) 365–388.
[38] J.A. Verheugen, H.P. Vijverberg, Intracellular Ca^{2+} oscillations and membrane potential fluctuations in intact human T lymphocytes: role of K^+ channels in Ca^{2+} signaling, Cell Calcium 17 (1995) 287–300.
[39] K.E. Barrett, Effect of the diglyceride lipase inhibitor, RG80267, on epithelial chloride secretion induced by various agents, Cell Signal 7 (1995) 225–233.
[40] L.D. Lawson, D.W. Powell, Bradykinin-stimulated eicosanoid synthesis and secretion by rabbit ileal components, Am. J. Physiol. 252 (1987) G783–G790.
[41] A. Wulf, A. Schwab, Regulation of a calcium-sensitive K^+ channel (cIK1) by protein kinase C, J. Membr. Biol. 187 (2002) 71–79.
[42] A.C. Gerlach, N.N. Gangopadhyay, D.C. Devor, Kinase-dependent regulation of the intermediate conductance, calcium-dependent potassium channel, hIK1, J. Biol. Chem. 275 (2000) 585–598.
[43] R. Jacob, Calcium oscillations in endothelial cells, Cell Calcium 12 (1991) 127–134.
[44] J.A.M. Borghans, G. Dupont, A. Goldbeter, Complex intracellular calcium oscillations. A theoretical exploration of possible mechanisms, Biophys. Chem. 66 (1997) 25–41.